Reversible pH-Responsive Fluorescence of Water-Soluble Polyfluorenes and Their Application in Metal Ion Detection

Lingling Li, Fang He,* Xiaoyu Wang, Ning Ma, and Lidong Li*

School of Materials Science and Engineering, University of Science and Technology Beijing, Beijing 100083, P. R. China

S Supporting Information

ABSTRACT: A novel water-soluble conjugated polymer poly{(4,4′-azobenzene)-2,7-[9,9-bis(6′-N,N,N,-trimethylammonium)hexyl fluorene]dibromide} (PFAB) has been designed and synthesized via Suzuki cross-coupling the fluorene units and azobenzene units. Through simple photoreduction, the azo group of the nonfluorescent PFAB to hydrazine group using UV light, polyfluorene PFAB-L with turn-on fluorescence in aqueous solution is obtained. The optical measurements illustrate that the generation of the flexible hydrazine group induces face-to-face arrangement of phenyl–fluorene–phenyl moieties. Therefore, the excimer formation of phenyl–fluorene–phenyl moieties was induced in PFAB-L. And the fluorescence of PFAB-L can be controlled through modulating the protonation of the −NH−NH− group in solution with different pH. The pH-responsive property is reversible. Moreover, the Fe^{3+} ions can selectively quench the fluorescence of the PFAB-L. This new polymer PFAB-L could be used for selective and sensitive sensing Fe^{3+} ions in aqueous solution.

KEYWORDS: *fluorescence, polyfluorene, excimer, photoreduction, pH-responsive, ion detection*
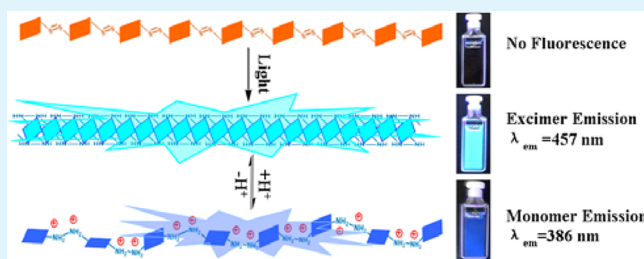
INTRODUCTION

Interaction between aromatic rings via π-stacking can affect the photophysical, electronic, and electrochemical properties of materials either in solution or in solid states. Controlled arrangement of π-conjugate groups or molecules is of great importance in organic materials science and biological chemistry. Therefore, molecular design and synthesis for ordering fabrication modulated by molecular crystalline properties, self-assembly, and supramolecular chemistry have been widely studied.[1−8]

Polyfluorene and derivatives have been widely studied for functional and practical applications such as sensors and electronic devices for their excellent chemical and physical properties, high blue light-emitting efficiency, and good thermal stability.[9−20] They also have been widely used for building π-stacking structure and self-assembly materials with unique properties. The backbone of blue light-emitting polyfluorenes are typically rigid and tend to aggregate, resulting in red-shifted emission. Moreover, excimeric emission has been found in polyfluorenes, which is always induced in films by interchain aggregation.[21−23] Control over the intrachain self-organization of polyfluorene derivatives to form strong and controllable intramolecular excimeric emission in solution has been rarely reported. A series of complex alkyl-substituted oligofluorenes that were induced to form a face-to-face structure were only reported to show strong excimeric emission in organic solvent.[24] However, excimer emission of polyfluorenes in aqueous solution has not been reported hitherto.

In this paper, we develop a novel water-soluble conjugated polymer poly{(4,4′-azobenzene)-2,7-[9,9-bis(6′-N,N,N,-trimethylammonium)hexyl fluorene]dibromide} (PFAB) via Suzuki cross-coupling the fluorene units and azobenzene units. Through simple photoreduction (the azo group of the nonfluorescent PFAB to flexible hydrazine group using UV light), reduced polyfluorene PFAB-L with strong and controllable excimeric emission in aqueous solution was prepared. Moreover, the excimer−monomer formation of PFAB-L can be controlled through modulating the protonation of the −NH−NH− group in solutions with different pH values.

Moreover, the obtained polymer PFAB-L had an interesting feature of highly selective and sensitive fluorescence quenching by Fe^{3+} ions. The Fe^{3+} ion is one of the most abundant metal ions in life forms. It involves a variety of fundamental physiologically processes in organisms and plays an important role in many biochemical processes.[25] Both the deficiency and excess of Fe^{3+} ions can induce many diseases such as skin ailments, various anemia, insomnia, kidney, and liver damage.[26−28] However, only few sensitive and selective fluorescent sensors for Fe^{3+} have been reported.[29−40] Therefore, we also prepared a new Fe^{3+} sensor using the novel polymer PFAB-L.

Scheme 1. (a) Synthesis Routine of Polymer PFAB and (b) Photoreduction and pH-Responsive Mechanism of PFAB
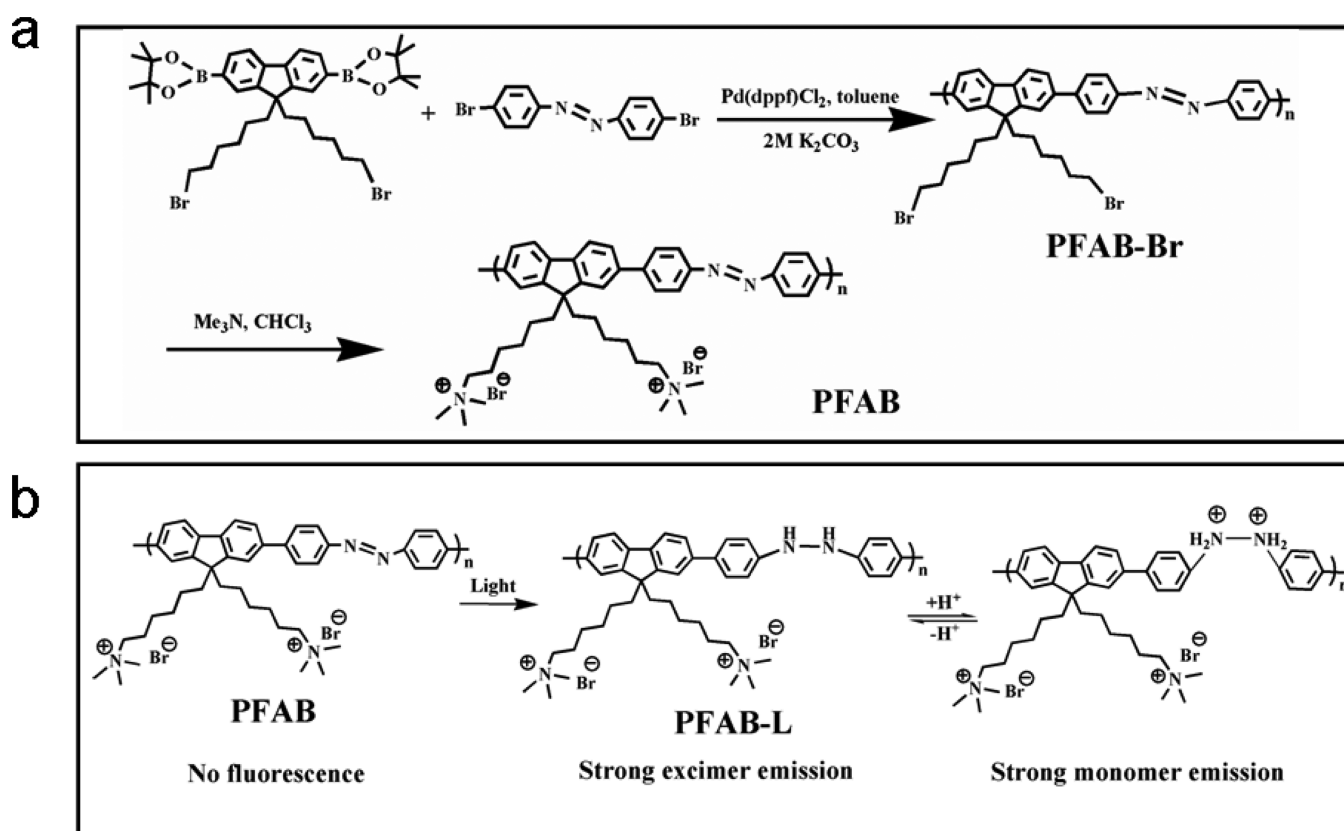
EXPERIMENTAL SECTION

Materials and Measurements. The compounds 2,2′-(9,9-bis(6-bromohexyl)-9H- fluorene-2,7-diyl)bis(4,4,5,5-tetramethyl-1,3,2-dioxaborolane)[41] and 1,4-dibromoazobenzene[42] were synthesized according to the procedure in the literature. The other materials were obtained from Alfa-Aesar. The ^1H NMR and ^{13}C NMR spectra were recorded on 400 MHz AC Bruker spectrometer. The UV−vis absorption spectra were taken on a Hitachi U-3900H spectrophotometer. The fluorescence spectra were measured with a Hitachi F-7000 spectrophotometer equipped with a Xenon lamp excitation source. FT-IR spectra were measured on a Bruker IF66v spectrophotometer. The gel permeation chromatography (GPC) analysis was performed on a Waters Styragel system using polystyrene as a calibration standard with THF as the eluent.

Synthesis of Poly[4,4′-azobenzene-2,7-(9,9-bis(6-dibromohexyl) fluorene)] (PFAB-Br). The monomers 2,2′-(9,9-bis(6-bromohexyl)-9H-fluorene-2,7-diyl)bis(4,4,5,5-tetramethyl-1,3,2-dioxaborolane) (372 mg, 0.5 mmol) and 1,4-dibromoazobenzene (170 mg, 0.5 mmol) were dissolved into 16 mL of toluene, and then, 4 mL of 2.0 M potassium carbonate was added. After degassing with nitrogen for 30 min, 10 mg of catalysis Pd(dppf)Cl$_2$ was added. The mixture was stirred at 80 °C for 48 h under nitrogen. The obtained solution was cooled down and extracted with CHCl$_3$. The organic layer was combined and dried over anhydrous MgSO$_4$. Then the solvent was removed, and the residue was dissolved in 2 mL of CHCl$_3$ and poured into 200 mL of acetone. Subsequently, the precipitate was collected by centrifugation. The precipitation process from CHCl$_3$ into acetone was repeated twice. The product was dried under vacuum to afford 280 mg of bright orange solid (yield 68%). ^1H NMR (400 MHz, CDCl$_3$, δ, ppm): 8.11−8.04 (br, 2H), 7.89−7.82 (br, 6H), 7.73−7.58 (br, 6H), 3.27 (tr, 4H), 2.12 (br, 4H), 1.68−1.62 (br, 4H), 1.26−1.09 (br, 8H), 0.77 (br, 4H). ^{13}C NMR (400 MHz, CDCl$_3$, δ, ppm): 152.0, 151.6, 150.7, 144.0, 141.2, 140.6, 139.4, 132.3, 127.8, 127.4, 127.0, 126.5, 125.3, 124.4, 123.6, 122.9, 121.4, 120.4, 55.4, 40.3, 33.9, 33.8, 29.1, 27.8, 23.7. M_w = 18493, M_n = 8198, PDI = 2.25.

Synthesis of Polymer PFAB. A 30% trimethylamine-alcohol solution (2 mL) was added into the solution of PFAB-Br (200 mg, 0.24 mmol) in CHCl$_3$ (50 mL) and stirred for 48 h at room temperature. Then, the solvent was removed by evaporation under vacuum. The residue was redissolved by 20 mL of methanol, and the solvent was removed again. The procedure was repeated five times. After being dried under vacuum, 230 mg of red solid PFAB was obtained.

Photoreduction Assay. A 250 μL portion of PFAB (1×10^{-4} M) solution was added into seven 1 cm × 1 mm quartz cuvettes. Then, the solutions were respectively irradiated for 0, 5, 8, 10, 11, 12, and 15 min with a 1000 W high-pressure mercury lamp, which was placed 25 cm away from the solution. After the irradiation, the absorption spectra of the samples were measured directly, and 30 μL portions of the solutions were dropped on the CaF$_2$ chip and dried for the FT-IR spectra measurements. Five microliter portions of the irradiated solutions (1×10^{-4} M) were diluted into 1 mL of H$_2$O in a 3 mL quartz cuvette, and the fluorescence spectra were measured, respectively.

pH-Responsive Property Assay. A 250 μL portion of PFAB (1×10^{-4} M) solution in PBS buffer at different pH values (2.0, 3.0, 4.0, 5.0, 6.0, 7.0, 10.0) was added into seven 1 cm × 1 mm quartz cuvettes, respectively. The absorption spectra of the samples were measured before and after irradiation for 15 min. Then, 5 μL of the PFAB-L (PFAB irradiated for 15 min, 1×10^{-4} M) solution was added into 1 mL of PBS buffer (25 mM) at different pH values for fluorescence spectra measurements. The pH of the buffers was adjusted with HCl (1 M) or NaOH (1 M) for the pH cycle experiments.

RESULTS AND DISSCUSSION

Synthesis and Characterization of PFAB. The chemical structure and the synthesis procedures of conjugated polymer PFAB are outlined in Scheme 1a. PFAB-Br was first obtained via Suzuki cross-coupling. Then PFAB-Br was treated with 30% trimethylamine solution for 48 h, and water-soluble conjugated

polymer PFAB was obtained. The absorption spectrum of PFAB-Br in $CHCl_3$ exhibits a broad peak at 415 nm and a much weaker absorption at 290 nm (Figure 1). The peak at 415
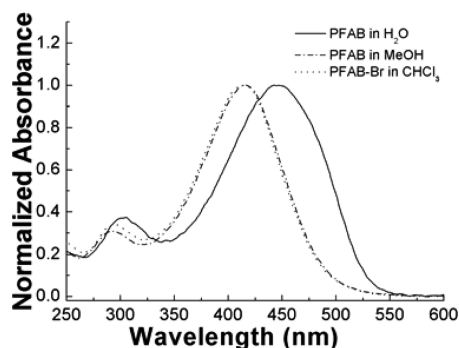
Figure 1. Normalized absorption spectra of PFAB in H_2O and in methanol, PFAB-Br in $CHCl_3$.

nm is associated with the $\pi-\pi*$ transition of the conjugated fluorene and azobenzene units. The absorption of PFAB in methanol is similar with PFAB-Br in $CHCl_3$. But the absorption of PFAB in H_2O is red-shifted to 445 nm by interchain aggregation. Neither PFAB-Br nor PFAB exhibit distinct fluorescence emission, which is similar to the case of previously reported conjugated polymers with azobenzene units in the main chain.[43]

Photoreduction of PFAB. It is well-known that the azo units can undergo a reversible cis−trans transition upon irradiation by the UV or visible light, which can result in the absorption spectrum being shifted. But for the copolymers PFAB-Br or PFAB, no obvious cis−trans transitions were observed after irradiation using conventional UV light for the highly rigid polymer chains hindered the photoisomerization. However, after irradiating the copolymers using a 1000 W high-pressure mercury lamp, we found that the azo (—N═N—) group of polymers was destroyed. However, for the high viscosity of the PFAB solution, the accurate chemical structure of PFAB before and after irradiation cannot be measured using NMR or even high-temperature NMR. Therefore, we try to verify the irradiation process of PFAB by the FT-IR spectra. As shown in Figure 2, a new band appeared at around 1520 cm^{-1}
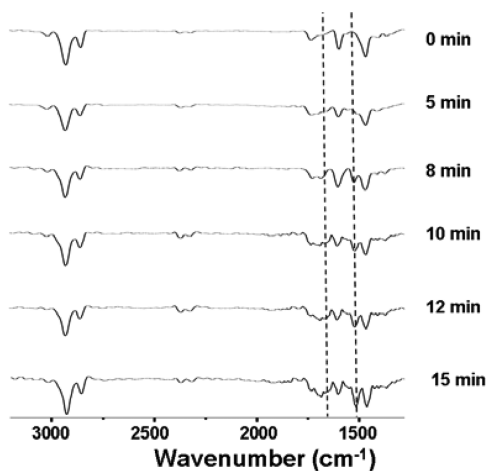
Figure 2. FT-IR spectra of PFAB in H_2O as a function of UV irradiation time.

and gradually increased in intensity with increase of irradiation time from 0 to 15 min. The band at 1520 cm^{-1}, which can be attributed to the bending vibration of the N—H group,[44] illustrated that the azobenzene moieties was reduced to its hydrazine derivative (—NH—NH—). Similar peaks attributed to N—H bending mode were also observed around 1514 cm^{-1} when the azobenzene (Ph—N═N—Ph) was reduced to hydrazobenzene moiety (Ph—NH—NH—Ph) by the electrochemistry method.[45−47] Moreover, the aromatic ring stretching band shifted from 1732 to 1675 cm^{-1} because of the variation in electron density and dipole moment around the rings after the formation of the electron-donor —NH—NH— group. The structure of PFAB was supposed to be changed to PFAB-L as shown in Scheme 1b.

Optical Properties of Copolymers after Irradiation. Then, we examined the optical properties of PFAB in aqueous solution and also of PFAB-Br in $CHCl_3$ solution before and after irradiation to verify the structures. Figure 3a shows absorption spectra of PFAB-Br ([PFAB-Br] = 1 × 10^{-4} M in RUs) in $CHCl_3$ solution as a function of irradiation time. Upon irradiation time up to 6 min, the absorption spectrum of PFAB-Br changed dramatically. The absorption peak was blue-shifted from 415 to 330 nm. Moreover, for the PFAB in aqueous solution, the variation was similar with the PFAB-Br. As shown in Figure 3b, the $\pi-\pi*$ transition peak of PFAB ([PFAB] = 1 × 10^{-4} M in RUs) at 445 nm was gradually decreased in intensity and blue-shifted upon irradiation for 15 min. Simultaneously, a new absorption at about 340 nm, which is associated with the phenyl−fluorene−phenyl moieties, gradually increased in intensity. The peak at 445 nm disappeared after irradiation for 15 min, which illustrated that the photoreduction time of PFAB was longer than that of PFAB-Br. The change of the absorption spectrum was opposite to the azobenzene trans−cis isomerization and indicated that the conjugation of polymers was disturbed by UV radiation.[48,49] In addition, a noticeable color change from yellow to colorless of polymer solutions after irradiation gave visible evidence of the destruction of the azo bond (inset in Figure 3a and b).

Accordingly, the fluorescence emission spectra of the copolymers as a function of irradiation time were also recorded. As shown in Figure 3c, a clear emission peak around at 388 nm was observed, which gradually increases in intensity after irradiation of PFAB-Br upon 0−4 min and then slightly decreases after irradiation from 4−6 min in $CHCl_3$ solution. The variation tendency of the emission spectrum was in good accordance with that of the absorption spectrum. This "turn-on" emission was due to the phenyl−fluorene−phenyl oligomers. This result demonstrated that the electron acceptor azo group has been destroyed.

Even more importantly, a unique emission change of PFAB solution was observed after irradiation. As shown in Figure 3d, the intensity of a large, structureless band with maximum at 457 nm, which exhibited a significantly different behavior from the emission spectra of fluorene derivatives, was dramatically increased when the irradiated solution was excited at 340 nm. The fluorescence of PFAB-L was observed to increase gradually and reach a maximum after 15 min, which was enhanced about 320 times after photoreduction. The fluorescence photographs of PFAB solution illustrated the strong "turn-on" cyan fluorescence after irradiation for 15 min (inset in Figure 3b). The emission peak of PFAB-L was red-shifted by about 70 nm compared to that of PFAB-Br-L, which was not simply caused by the aggregation of the polymers. By comparison with
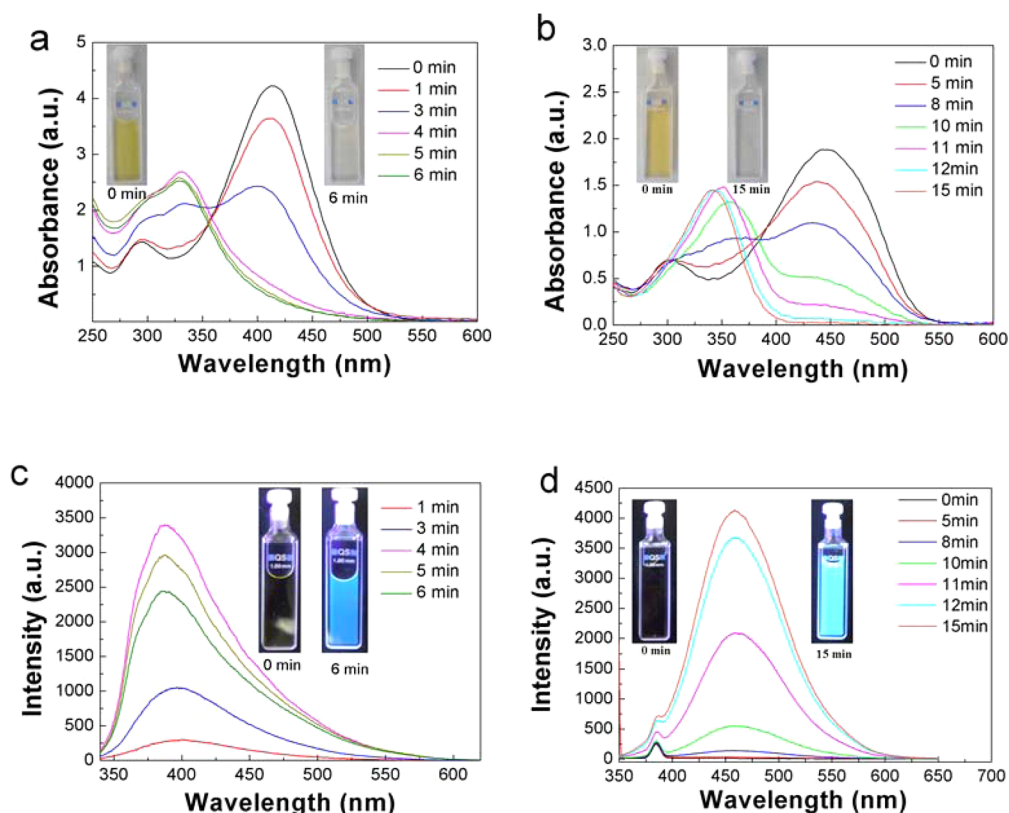
Figure 3. Absorption spectra of (a) PFAB-Br in CHCl$_3$ solution and (b) PFAB in aqueous solution as a function of UV irradiation time, [PFAB-Br] = 1 × 10^{-4} M and [PFAB] = 1 × 10^{-4} M in repeating units (RUs). Emission spectra of (c) PFAB-Br in CHCl$_3$ solution and (d) PFAB in H$_2$O as a function of UV irradiation time, [PFAB-Br] = 5 × 10^{-7} M and [PFAB] = 5 × 10^{-7} M in RUs. The excitation wavelength is 340 nm. (insets) (a and b) Photographs and (c and d) fluorescence photographs of PFAB-Br and PFAB solution before and after irradiation.
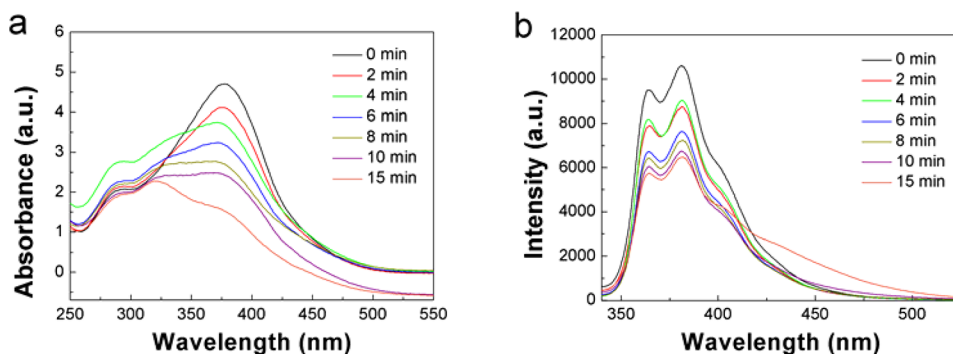

Figure 4. (a) Absorption spectra and (b) emission spectra of OFAB in H$_2$O as a function of irradiation time; [OFAB] = 1 × 10^{-4} M for absorption spectra; [OFAB] = 5 × 10^{-7} M for emission spectra. The excitation wavelength is 330 nm.

reported intramolecular excimer emissions of fluorene derivatives,[21−23] we supposed that the large band was assigned to intramolecule excimeric emission of phenyl−fluorene−phenyl moieties. The azo (—N≡N—) group of PFAB was photoreduced to its hydrazine derivative (—NH—NH—) in aqueous solution. The formation of the flexible —NH—NH— group induces the phenyl−fluorene−phenyl moieties in the polymer chain to a face-to-face arrangement via π−π stacking interaction,[50−52] causing the intramolecular excimeric emission. From the results of PFAB-Br and PFAB, we found that the self-organization of phenyl−fluorene−phenyl moieties can only be induced in aqueous solution.

Optical Properties of Model Oligomer after Irradiation. From the previous research, there is another possibility

for the green emission at 457 nm of polyfluorene derivatives, the keto defects in polyfluorene backbone.[53,54] Therefore, in order to clarify the above spectral property, model oligomer OFAB was synthesized and irradiation experiments were performed to confirm the structure change. The chemical structure and the synthesis procedures of OFAB are illustrated in Figure S1 in the Supporting Information (SI). Figure 4a illustrates the UV−vis absorption spectrum of OFAB ([OFAB] = 1 × 10^{-4} M) as a function of irradiation time. It showed that before irradiation the absorption spectrum of OFAB in H$_2$O exhibited a broad peak at 378 nm and a much weaker absorption at 290 nm. The peak was blue-shifted about 67 nm compared with PFAB for the reduction of the conjugation length. After irradiation, the intensity of the peak at 378 nm of
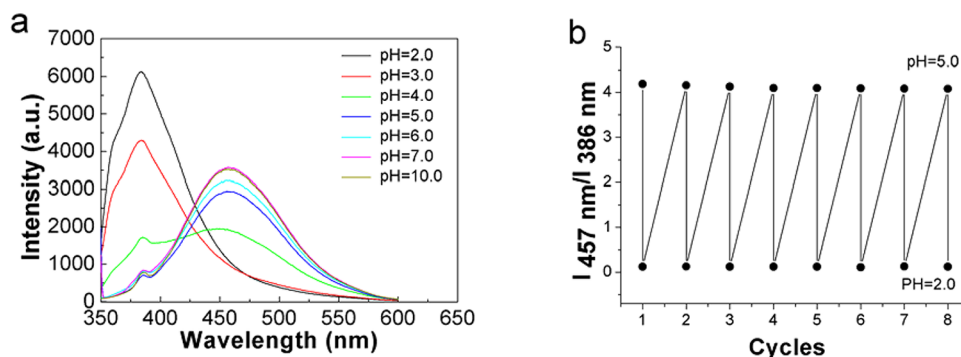
Figure 5. (a) Emission spectra of PFAB-L in PBS buffer (25 mM) as a function of pH, [PFAB-L] = 5×10^{-7} M in RUs. The excitation wavelength was 340 nm. (b) Emission intensity ratio I_{457nm}/I_{386nm} upon cycling the pH between 5 and 2.
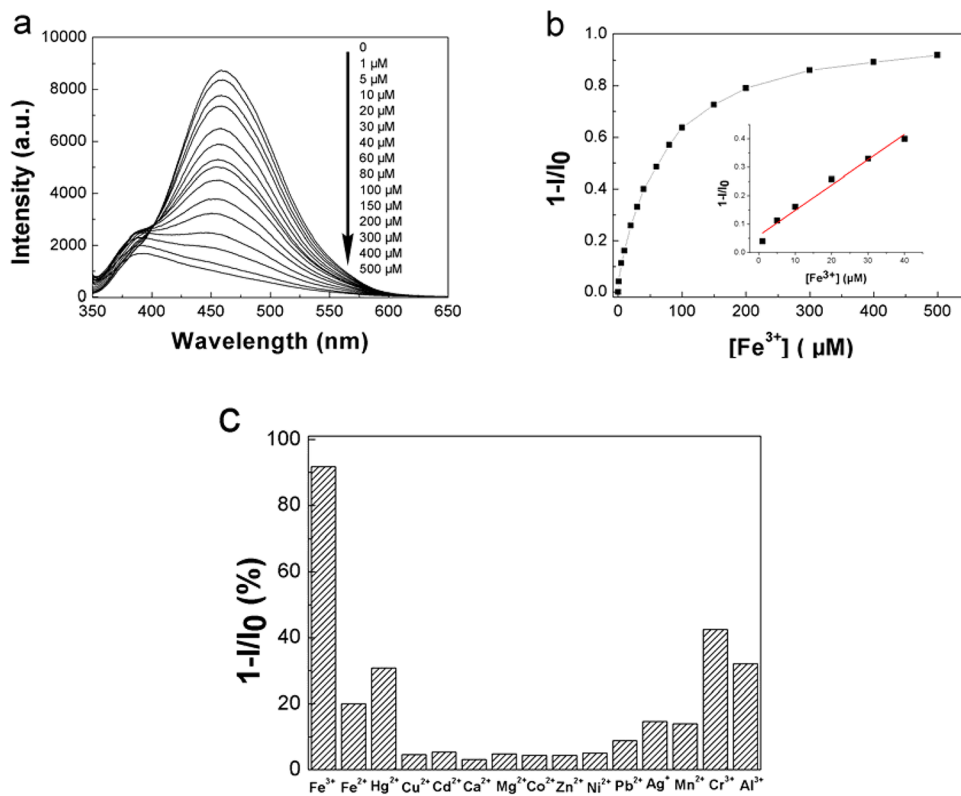
Figure 6. (a) Fluorescence emission spectra of PFAB-L in aqueous solution with successive addition of Fe^{3+}. (b) Fluorescence quenching efficiencies of PFAB-L as a function of Fe^{3+} concentration. (c) Fluorescence quenching efficiencies of PFAB-L in the presence of various ions. [PFAB-L] = 1.25×10^{-6} M in RUs, [ions] = 5.0×10^{-4} M, and the excitation wavelength is 340 nm.

OFAB was gradually decreased as the increase of the irradiation time, and the peak was gradually shifted to 320 nm. The UV−vis change of OFAB was similar with the change of PFAB-Br and PFAB. Then the ^{1}H NMR spectra of OFAB before and after irradiation were measured in CD_3OD. As shown in Figure S2 in the SI, after irradiation the proton signals of benzene near the azo unit at 8.05 and 7.93 ppm were shifted to about 7.54 ppm for the electron acceptor —N=N— change to electron donor —NH—. However, the proton signal of the active —NH— group cannot be observed maybe for low signal in CD_3OD. Moreover, all of the proton signals of fluorene units and side alkyl chain were not shifted. The results illustrated that the azo group was changed and the structure of fluorene units was unchanged. The ESI-MS spectra of OFAB before and after irradiation also supports this conclusion (Figure S3 in the SI).

Correspondingly, the emission spectra of OFAB were also changed after irradiation. Unlike PFAB, OFAB itself exhibited strong fluorescence emission at 364 and 381 nm. As shown in Figure 4b, the emission intensity of OFAB was gradually decreased as the increase of the irradiation time from 0 to 15 min. The fluorescence was quenched about 38% after irradiation for 15 min, but no new emission peak was observed. Moreover, water-soluble polyfluorene derivative PFP without azo group was also irradiated and studied. The structure of PFP was illustrated in the inset of Figure S4a in the SI. Figure S4a showed the absorption spectra of PFP as a function of irradiation time. Upon irradiation, the absorbance of the PFP was slightly decreased, but no peak shift was observed. The emission spectra in Figure S4b showed that the emission intensity of PFP was mildly quenched as the irradiation and no new peak was observed at 457 nm. The results showed that the

irradiation cannot defect the structure of fluorene units. Therefore, the possibility of the strong emission at 457 nm of PFAB-L originated from keto defects was excluded.

pH-Responsive Fluorescence of PFAB-L. Moreover, in this polymer, the formation of hydrazine group and excimeric formation was also supported by the pH-responsive fluorescence of PFAB-L in aqueous medium. Emission spectra of PFAB-L (5×10^{-7} M in RUs) as a function of pH were recorded in 25 mM PBS buffer. As shown in Figure 5a, at pH > 5 the phenyl–fluorene–phenyl moieties of PFAB-L were linked with flexible and neutral –NH–NH– groups, PFAB-L showed strong excimer fluorescence at 457 nm. There was little change in the intensity or shape of the emission spectrum when the pH decreased from 10 to 5. However, after the NH group was protonated to cationic $-NH_2^+$ group in acidic solution, the electrostatic repulsion interaction of $-NH_2^+-NH_2^+-$ linkers would disturb the excimer emission and increase the monomer emission of phenyl–fluorene–phenyl at 386 nm. Moreover, the intensity of the monomer emission increased with the protonation of –NH–NH– group, which was because the unprotonated amines are efficient electron-transfer quencher of the excited chromophores.[55] Therefore, when pH changes from 2 to 10, the quantum yields of the polymer were 17.8%, 10.5%, 7.2%, 7.9%, 7.4%, 7.5%, and 7.6%, respectively. When the pH changed from 5 to 2, the emission intensity of excimer at 457 nm decreased 3.6-fold and that of the monomer at 386 nm increased 8-fold, resulting in an overall 25-fold ratiometric (I_{457nm}/I_{386nm}) response. Furthermore, as shown in Figure 5b, the excimer–monomer emission changes of PFAB-L as a function of pH showed good reversibility.

Fe^{3+} Detection Using PFAB-L. Then, we detected the fluorescence of PFAB-L after addition of Fe^{3+} ions. Figure 6a shows the emission spectra of PFAB-L ([PFAB-L] = 1.25×10^{-6} M in RUs) upon gradually addition of Fe^{3+} ions ($0-5 \times 10^{-4}$ M). Titrating aqueous solution of Fe^{3+} salt led to a significant quenching of the PFAB-L fluorescence. The quenching of PFAB-L shows a nonlinear curvature at higher Fe^{3+} ion concentrations (Figure 6b). And a linear Stern–Volmer plot is obtained with a Stern–Volmer constant (K_{sv}) of 8.9×10^3 M^{-1} at a lower Fe^{3+} concentration ($0-4 \times 10^{-5}$ M). For the conventional metal ions sensors based on quenching fluorescence, the mechanism almost due to combination factors such as electron transfer, delocalization of excitons, and competent energy migration along the polymer chain.[56−58] In this system, the monomer emission of PFAB-L appeared when 8×10^{-5} M of Fe^{3+} ion were added, and the 386 nm peak also decreased with the increase of Fe^{3+} concentration. When the concentration of Fe^{3+} ion reaches 4×10^{-4} M, the fluorescence intensity of PFAB-L is quenched up to 90%. The emission peak at 457 nm almost disappeared, and the peak at 386 nm also gradually quenched. Therefore, herein the association between Fe^{3+} and the NH–NH group disturbs the face-to-face $\pi-\pi$ stacking interaction and also facilitates the efficient electron transfer, resulting in high fluorescence quenching.

To study the specific interaction of PFAB-L with Fe^{3+} ions, various other ions are investigated under identical conditions. Figure 5c shows the fluorescence quenching efficiency of PFAB-L in the presence of Fe^{2+}, Hg^{2+}, Cu^{2+}, Cd^{2+}, Ca^{2+}, Mg^{2+}, Co^{2+}, Zn^{2+}, Ni^{2+}, Pb^{2+}, Ag$^+$, Mn^{2+}, Al^{3+}, and Cr^{3+} ions. It shows that PFAB-L is highly selective for Fe^{3+} ions. Although fluorescence quenching is detected upon addition of other ions, the value of the fluorescence quenching efficiency of PFAB-L for Fe^{3+} ions is over 2−21 times higher than those for

other ions. Moreover, trivalent ions Al^{3+} or Cr^{3+} show obvious fluorescence quenching to PFAB-L, and the value of the fluorescence quenching efficiency of PFAB-L for Fe^{3+} ions is over 2 times higher than those for Al^{3+} and Cr^{3+} ions. These results indicate that other trivalent ions have some effect on the fluorescence quenching of PFAB-L, but they also show good recognition ability for the Fe^{3+} ions of PFAB-L.

■ CONCLUSION

In summary, a novel water-soluble polyfluorene PFAB-L with strong excimer emission is obtained. PFAB-L is simply prepared by photoreduction the azo group of nonfluorescent PFAB. The rigid azo group of PFAB is reduced to the flexible –NH–NH– group and induced a face-to-face arrangement of phenyl–fluorene–phenyl moieties, resulting in "turn-on" of strong excimer fluorescence at 457 nm in aqueous solution. The fluorescence of PFAB-L reversibly responds to pH in aqueous solution owing to protonation of the –NH–NH– group. Furthermore, PFAB-L was utilized for sensitive and selective detection Fe^{3+} in aqueous solution. These significant and unique properties of PFAB-L will certainly inspire fundamental development of new materials for chemsensors and biosensors.

■ ASSOCIATED CONTENT

ⓢ Supporting Information
Scheme of synthesis route of OFAB, synthesis procedure of OFAB, photoreduction assay procedure of OFAB, ^{1}H NMR spectra and ESI-MS of OFAB before and after irradiation, chemical structure of PFP, absorption and emission spectra of PFP before and after irradiation. This material is available free of charge via the Internet at http://pubs.acs.org.

■ AUTHOR INFORMATION

Corresponding Author
*E-mail: lidong@mater.ustb.edu.cn (L.L.); hefang@mater.ustb.edu.cn (F.H.).
Notes
The authors declare no competing financial interest.

■ ACKNOWLEDGMENTS

■ REFERENCES

(1) DiBenedetto, S. A.; Facchetti, A.; Ratner, M. A.; Marks, T. J. *Adv. Mater.* **2009**, *21*, 1407−1433.
(2) Wouters, D.; Hoeppener, S.; Schubert, U. S. *Angew. Chem., Int. Ed.* **2009**, *48*, 1732−1739.
(3) Hirst, A. R.; Escuder, B.; Miravet, J. F.; Smith, D. K. *Angew. Chem., Int. Ed.* **2008**, *47*, 8002−8018.
(4) Yashima, E.; Maeda, K.; Iida, H.; Furusho, Y.; Nagai, K. *Chem. Rev.* **2009**, *109*, 6102−6211.
(5) Cheng, Y. J.; Yang, S. H.; Hsu, C. S. *Chem. Rev.* **2009**, *109*, 5868−5923.
(6) Boussicault, F.; Robert, M. *Chem. Rev.* **2008**, *108*, 2622−2645.
(7) Szacilowski, K. *Chem. Rev.* **2008**, *108*, 3481−3548.
(8) Babu, S. S.; Möhwald, H.; Nakanishi, T. *Chem. Soc. Rev.* **2010**, *39*, 4021−4035.

(9) Zhu, C. L.; Liu, L. B.; Yang, Q.; Lv, F. T.; Wang, S. *Chem. Rev.* **2012**, *112*, 4687−4735.

(10) He, F.; Liu, L. B.; Li, L. D. *Adv. Funct. Mater.* **2011**, *21*, 3143−3149.

(11) Feng, X. L.; Liu, L. B.; Wang, S.; Zhu, D. B. *Chem. Soc. Rev.* **2010**, *39*, 2411−2419.

(12) Xing, C. F.; Shi, Z. Q.; Yu, M. H.; Wang, S. *Polymer* **2008**, *49*, 2698−2703.

(13) Thomas, S. W.; Joly, G. D.; Swager, T. M. *Chem. Rev.* **2007**, *107*, 1339−1386.

(14) Yu, M. H.; He, F.; Tang, Y. L.; Wang, S.; Li, Y. L.; Zhu, D. B. *Macromol. Rapid Commun.* **2007**, *28*, 1333−1338.

(15) Liu, B.; Bazan, G. C. *Proc. Natl. Acad. Sci. U.S.A.* **2005**, *102*, 589−593.

(16) Wang, S.; Gaylord, B. S.; Bazan, G. C. *J. Am. Chem. Soc.* **2004**, *126*, 5446−5451.

(17) Ariu, M.; Lidzey, D. G.; Lavrentiev, M.; Bradley, D. D. C.; Jandke, M.; Strohriegl, P. *Synth. Met.* **2001**, *116*, 217−221.

(18) Neher, D. *Macromol. Rapid Commun.* **2001**, *22*, 1365−1385.

(19) Scherf, U.; List, E. J. W. *Adv. Mater.* **2002**, *14*, 477−487.

(20) Chen, X.; Liao, J. L.; Liang, Y.; Ahmed, M. O.; Tseng, H. E.; Chen., S. A. *J. Am. Soc. Chem.* **2003**, *125*, 636−637.

(21) Pei, Q.; Yang, Y. *J. Am. Chem. Soc.* **1996**, *118*, 7416−7417.

(22) Lu, H. H.; Liu, C. Y.; Jen, T. H.; Liao, J. L.; Tseng, H. E.; Huang, C. W.; Hung, M. C.; Chen, S. A. *Macromolecules* **2005**, *38*, 10829−10835.

(23) Kwon, Y. K.; Kim, H. S.; Kim, H. J.; Oh, J. H.; Park, H. S.; Ko, Y. S.; Kim, K. B.; Kim, M. S. *Macromolecules* **2009**, *42*, 887−891.

(24) Thirion, D.; Poriel, C.; Barrière, F.; Métivier, R.; Jeannin, O.; Rault-Berthelot, J. *Org. Lett.* **2009**, *11*, 4794−4797.

(25) Eisenstein, R. S. *Annu. Rev. Nutr.* **2000**, *20*, 627−662.

(26) Touati, D. *Arch. Biochem. Biophys.* **2000**, *373*, 1−6.

(27) Matzanke, B. F.; Matzanke, G. M.; Raymond, K. N. *Iron Carriers and Iron Proteins*; VCH Publishers: New York, 1989; Vol. 5, p 1−121.

(28) Brugnara, C. *Clin. Chem.* **2003**, *49*, 1573−1578.

(29) Weizman, H.; Ardon, O.; Mester, B.; Libman, J.; Dwir, O.; Hadar, Y.; Chen, Y.; Shanzer, A. *J. Am. Chem. Soc.* **1996**, *118*, 12368−12375.

(30) Nudelman, R.; Ardon, O.; Hadar, Y.; Chen, Y.; Libman, J.; Shanzer, A. *J. Med. Chem.* **1998**, *41*, 1671−1678.

(31) Lee, T. S.; Yang, C.; Park, W. H. *Macromol. Rapid Commun.* **2000**, *21*, 951−955.

(32) Ma, Y.; Luo, W.; Quinn, P. J.; Liu, Z.; Hider, R. C. *J. Med. Chem.* **2004**, *47*, 6349−6362.

(33) Bricks, J. L.; Kovalchuk, A.; Trieflinger, C.; Nofz, M.; Büschel, M.; Tolmachev, A. I.; Daub, J.; Rurack, K. *J. Am. Chem. Soc.* **2005**, *127*, 13522−13529.

(34) Xiang, Y.; Tong, A. J. *Org. Lett.* **2006**, *8*, 1549−1552.

(35) Zhang, M.; Gao, Y.; Li, M.; Yu, M.; Li, F.; Li, L.; Zhu, M.; Zhang, J.; Yi, T.; Huang, C. *Tetrahedron Lett.* **2007**, *48*, 3709−3712.

(36) Mansell, D.; Rattray, N.; Etchells, L. L.; Schwalbe, C. H.; Blake, A. J.; Bichenkova, E. V.; Bryce, R. A.; Barker, C. J.; Díaz, A.; Kremerf, C.; Freeman, S. *Chem. Commun.* **2008**, *41*, 5161−5163.

(37) Zhang, T.; Fan, H.; Liu, G.; Jiang, J.; Zhou, J.; Jin, Q. *Chem. Commun.* **2008**, *42*, 5414−5416.

(38) Wu, X.; Xu, B.; Tong, H.; Wang, L. *Macromolecules* **2010**, *43*, 8917−8923.

(39) Saikia, G.; Iyer, P. K. *Macromolecules* **2011**, *44*, 3753−3758.

(40) Dwivedi, A. K.; Saikia, G.; Iyer, P. K. *J. Mater. Chem.* **2011**, *21*, 2502−2507.

(41) Stork, M.; Gaylord, B. S.; Heeger, A. J.; Bazan, G. C. *Adv. Mater.* **2002**, *14*, 361−366.

(42) Barakat, M. A.; Abdel-Wahab, M. F.; El-Sadr, M. M. *J. Chem. Soc.* **1956**, *0*, 4685−4687.

(43) Izumi, A.; Teraguchi, M.; Nomura, R.; Masuda, T. *J. Polym. Sci., Part A: Polym. Chem.* **2000**, *38*, 1057−1063.

(44) Yu, H.; Zhang, H.; Liu, Z. *Langmuir* **1998**, *14*, 619−624.

(45) Wang, R.; Iyoda, T.; Tryk, D. A.; Hashimoto, K.; Fujishima, A. *Langmuir* **1997**, *13*, 4644−4651.

(46) Yu, H. Z.; Zhang, H. L.; Liu, Z. F. *Langmuir* **1998**, *14*, 619−624.

(47) Yu, H. Z.; Ye, S.; Zhang, H. L.; Uosaki, K.; Liu, Z. F. *Langmuir* **2000**, *16*, 6948−6954.

(48) Haberhauer, G.; Kallweit, C. *Angew. Chem., Int. Ed.* **2010**, *49*, 2418−2421.

(49) Winnik, F .M. *Chem. Rev.* **1993**, *93*, 587−614.

(50) Zhang, X.; Rehm, S.; Safont-Sempere, M. M.; Würthner, F. *Nat. Chem.* **2009**, *1*, 623−629.

(51) Shiraishi, Y.; Tokitoh, Y.; Hirai, T. *Org. Lett.* **2006**, *8*, 3841−3844.

(52) Shiraishi, Y.; Tokitoh, Y.; Nishimura, G.; Hirai, T. *Org. Lett.* **2005**, *7*, 2611−2614.

(53) Bliznyuk, V. N.; Carter, S. A.; Scott, J. C.; Klärner, G.; Miller, R. D.; Miller, D. C. *Macromolecules* **1999**, *32*, 361−369.

(54) Gaal, M.; List, E. J. W.; Scherf, U. *Macromolecules* **2003**, *36*, 4236−4237.

(55) Czarnik, A. W. *Fluorescent chemosensors for ion and molecular recognition*; American Chemical Society: Washington DC, 1993; Vol. 538, p 104−129.

(56) Bredas, J. L.; Cornil, J.; Beljonne, D.; Dos Santos, D. A.; Shuai, Z. *Acc. Chem. Res.* **1999**, *32*, 267−276.

(57) Nguyen, T. Q.; Wu, J.; Doan, V.; Schwartz, B. J.; Tolbert, S. H. *Science* **2000**, *288*, 652−656.

(58) Jones, R. M.; Bergstedt, T. S.; McBranch, D. W.; Whitten, D. G. *J. Am. Chem. Soc.* **2001**, *123*, 6726−6727.

4933

dx.doi.org/10.1021/am301286q | *ACS Appl. Mater. Interfaces* 2012, 4, 4927−4933